water

MDPI

Article

Water Balance and Level Change of Lake Babati, Tanzania: Sensitivity to Hydroclimatic Forcings

René P. Mbanguka [1,*], Steve W. Lyon [1], Karin Holmgren [1,2], Marc Girons Lopez [3] and Jerker Jarsjö [1]

1 Department of Physical Geography, and the Bolin Centre for Climate Research, Stockholm University, SE-106 91 Stockholm, Sweden; steve.lyon@su.se (S.W.L.); karin.holmgren@slu.se (K.H.); jerker.jarsjo@natgeo.su.se (J.J.)

2 Department of Urban and Rural Development, Swedish University of Agricultural Sciences, Box 7012, SE-750 07 Uppsala, Sweden

3 Department of Earth Sciences, Uppsala University, SE-752 36 Uppsala, Sweden; marc.girons_lopez@geo.uu.se

* Correspondence: rene.mbanguka@natgeo.su.se; Tel.: +46-739-984-937

Academic Editor: Karl-Erich Lindenschmidt

Received: 29 September 2016; Accepted: 28 November 2016; Published: 5 December 2016

Abstract: We develop and present a novel integrated water balance model that accounts for lake water—groundwater interactions, and apply it to the semi-closed freshwater Lake Babati system, Northern Tanzania, East Africa. The model was calibrated and used to evaluate the lake level sensitivity to changes in key hydro-climatic variables such as temperature, precipitation, humidity and cloudiness. The lake response to the Coupled Model Intercomparison Project, Phase 5 (CMIP5) output on possible future climate outcomes was evaluated, an essential basis in understanding future water security and flooding risk in the region. Results show high lake level sensitivity to cloudiness. Increased focus on cloud fraction measurement and interpretation could likely improve projections of lake levels and surface water availability. Modelled divergent results on the future (21st century) development of Lake Babati can be explained by the precipitation output variability of CMIP5 models being comparable to the precipitation change needed to drive the water balance model from lake dry-out to overflow; this condition is likely shared with many other East African lake systems. The developed methodology could be useful in investigations on change-driving processes in complex climate—drainage basin—lake systems, which are needed to support sustainable water resource planning in data scarce tropical Africa.

Keywords: Lake Babati; water balance; lake level sensitivity; cloudiness; hydroclimatic forcings; East Africa

1. Introduction

Hydrological modeling of lake systems enhances our understanding of important processes controlling lake dynamics. It also allows for quantified assessment of the impacts of future climatic and anthropogenic changes on water availability and of the functioning of aquatic ecosystems. East African lakes have long been the subject of many hydrological modeling studies, mainly for the purpose of estimating their water budgets and their sensitivity to climatic forcings. Examples include the modeling of Lake Victoria's water balance with specific emphasis on the evolution of its water storage and the impacts of climatic changes and human management on the lake outflow [1–3]; modeling of water level fluctuations and estimation of surface evaporation at the shallow Lake Ziway (Ethiopia) [4]; assessing the sensitivity of Lake Tana (Ethiopia) to changes in rainfall [5]; and modeling the water balance of Lake Manyara (Tanzania) [6]. Hydrological modeling studies of lakes in the East African region have also aimed at improving the reconstruction of paleoclimatic conditions inferred from

climate proxies such as fossil pollen and diatoms in lake sediments. For example, modeling the paleo-lake levels of Lake Naivasha and mega-lake Suguta (Kenya) allowed the validation of estimates of paleo-precipitation in East Africa [7,8].

Many of these lake-centric hydrological modelling studies have involved isolating the lake body from its surrounding catchment area; whereby catchment inputs are estimated independently and fed into the lake model. For example, [9] coupled their Lake Abiyata (Ethiopia) water balance model with surface inflow calculated using a catchment runoff model and applied groundwater fluxes estimated with a numerical groundwater flow model. Drawbacks of this de-coupled approach are that lake interactions with catchment processes and conditions, such as lake level—groundwater level interactions, are neglected, and that uncertainties inherent in various methods of estimating these internal fluxes are transferred into the lake model. Such uncertainties can make closing the water balance difficult, leading to relatively large discrepancies of the lake water balance [6]. In addition, these uncertainties can compound into an unrealistic calibration of model parameters or other water balance components.

Another challenge to the successful modelling of lake systems is the difficulty to reasonably estimate lake evaporation, which is often the largest component of lake water budget [7]. Indeed, lake evaporation cannot be easily measured and its calculation requires large amounts of location-specific data, which is typically not available in most remote areas of Africa or is only available through regional-scale databases (i.e., [10]). For example, lake surface evaporation can be sensitive to changes in cloudiness [3,11] but many lake modelling studies in the region have rarely considered this parameter in their estimates. Further, since lake systems, especially closed ones, tend to be dynamic over the course of the year and between years, they are particularly sensitive to climatic forcings both over the lake and within the surrounding catchment (e.g., [12]). While many of the available studies have been able to assess the sensitivity of lake systems to climatic changes, this is typically done to constrain parameter uncertainties and their contributions to model predictions. However, there is little documentation (e.g., [2]) of studies on future lake system changes based on actual projections from global circulation models in the region.

In this study, we present a novel water balance model of the semi-closed fresh water Lake Babati, Northern Tanzania. The lake supplies water to meet the various needs of the about one hundred thousand citizens in Babati town [13] and supports a diverse ecosystem, including between seventy and ninety hippos and several species of fish and lake birds [14,15]. Furthermore, like most of the neighbouring lakes [16–19], Lake Babati could be equally rich in proxy climate data, which is essential for local and regional paleoclimatic studies. A combination of extensive landscape changes in the lake's catchment and recurrent extreme precipitation events over the last century has triggered frequent lake flooding events, inundating Babati town, which is located at the downstream of the lake outlet [20]. The ever-increasing population density around the lake and prospective impacts of regional climate change and variability also pose a serious threat to the sustainability of the lake water resources. Despite its importance, the general hydrology of the lake remains little known. Previous efforts [21] have developed a lumped lake-centric water balance model to simulate the lake levels and flood discharge, based on daily rainfall, surface and groundwater fluxes, groundwater storage and evapotranspiration. The model, however, presented large uncertainties, since the approach did not allow consideration of water balance constraints imposed on the estimated fluxes by the lake catchment.

As such, the water balance model presented in this study is based on a rather novel approach of considering the lake and its catchment together in a truly integrated implementation. This allows highly uncertain fluxes, such as the groundwater discharge into the lake, to be adequately constrained through closure of overall water balances. Together, this coupled groundwater–lake water approach can provide a robust method to estimate lake level and volume changes in a data-scarce setting. With that, the purpose of the study is to evaluate the lake level sensitivity to climatic variables that may change in the future as a result of global climate change, such as temperature, precipitation, humidity

and cloudiness, and response to future scenarios of climatic forcings. More generally, such knowledge is essential in assessments of future water security (e.g., surface water availability) and flooding risks.

2. Materials and Methods

2.1. Description of the Study Site

2.1.1. General

Lake Babati is located at approximately 35°45′ E and 4°15′ S about 200 km to the South West of the city of Arusha in northern Tanzania (Figure 1). It is a fresh water lake, with relatively shallow but highly fluctuating water levels [14]. The lake may have been formed following the East African Rift Valley floor uplift that resulted in the creation of both temporary and permanent lakes in the region, including the neighbouring Lake Manyara or Lake Burungi [22].

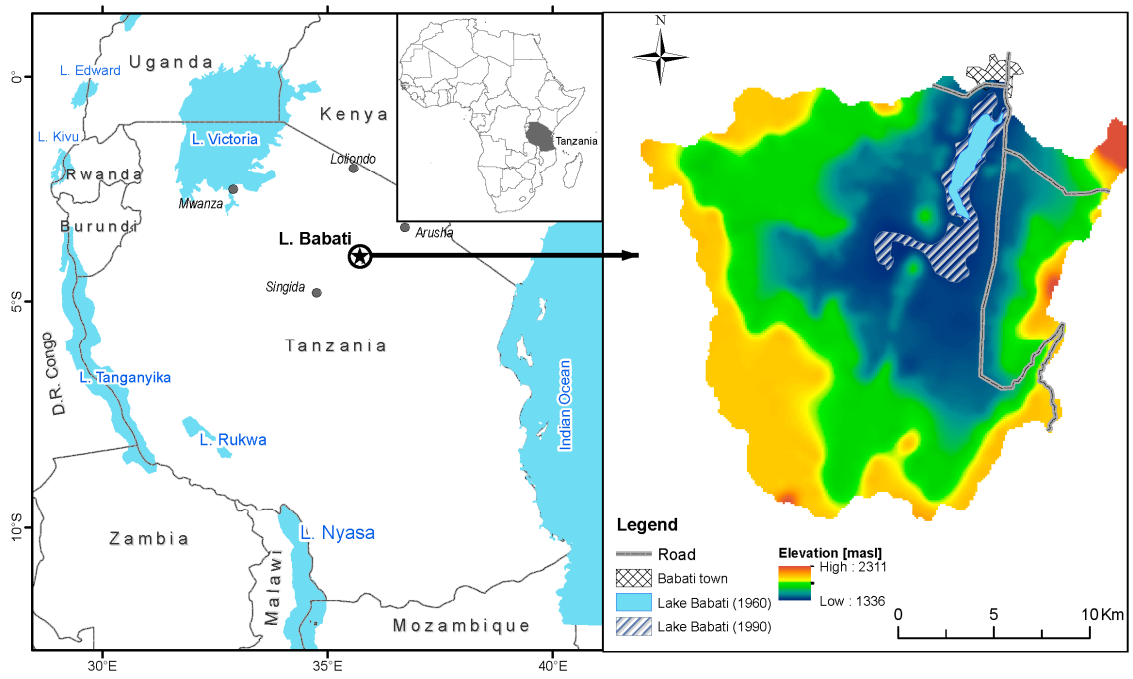

Figure 1. Location of Lake Babati (**left**); and the Lake and its catchment area (**right**).

The lake is located at an altitude of 1345 mean above sea level (m a.s.l.). It has a current average surface area of 7 km^2 and its hydrological catchment covers about 355 km^2. The ratio of the lake to basin area has increased from 0.013 in 1960 to 0.02 in 1990. The catchment area can be subdivided into two geomorphologically distinct areas: the southern part, consisting of a steep landscape with hills and plateaux formed by Precambrian basement rocks; and the northern part, dominated by a volcanic landscape, where neogene volcanic deposits in the shape of pyroclasts and minor explosion vents and craters form the major features [20]. The area close to the lake is surrounded by wide plains of *mbugas*—black cotton soils [23] and clear sands. Large sandfans are observed upstream from the *mbugas* creating a large water infiltration area covering approximately 50 km^2. Large-scale gully erosion takes place in the volcanic soils to the North and forms a well-developed drainage system that transports sediments into the alluvial sands and *mbugas* around the lake. At the northern downstream edge of the lake is Babati town, lying on a volcanic tuff ridge with dark brown soils, which is highly erodible and susceptible to infiltration. Groundwater flow from the lake has been observed through this feature and supports valley cultivation to the east of the town [20].

The lake's catchment has been used as grazing land since at least 2000 years ago [24]. The catchment was mostly dominated by forests, with agriculture occupying a small fraction at the beginning of the twentieth century [21,25], but due to the land management policy implemented in the 1970s, considerable parts of the forest have been converted into farmlands [21]. It has been suggested [26] that while there was still more bushland or woodland than cultivated areas in 1960s, cultivated land doubled the combined bushland and woodlands area in the 1990s.

2.1.2. Hydroclimatic Conditions and Independent Observations of Water Balance Components

The region experiences two rainy seasons between October and May, separated by a short dry spell (January–February), with the rest of the year consisting of a dry season [20,27]. Records from Babati meteorological station between 1973 and 2009 indicate that the area receives an average rainfall of 789 mm per year, with a standard deviation of 278 mm (Figure 2). The data poorly correlates with records of neighbouring stations, such as Galappo Mission (13 km), Mulu (45 km) and Haubi Mission (63 km), indicating a complex spatial distribution of rainfall in the region ([20,21,28]). Previous work [27] suggests that the region is subject to large regional inter-annual variations in rainfall due to the El Niño-Southern Oscillation (ENSO) as well as orographically induced precipitation in the highlands. Rainfall records around the study area indicate that the topographic effect is 3.6 mm/year/100 m, explaining a relatively modest percentage (4%) of total rainy season precipitation between stations. The annual average temperature is 19.4 °C observed over the same period.

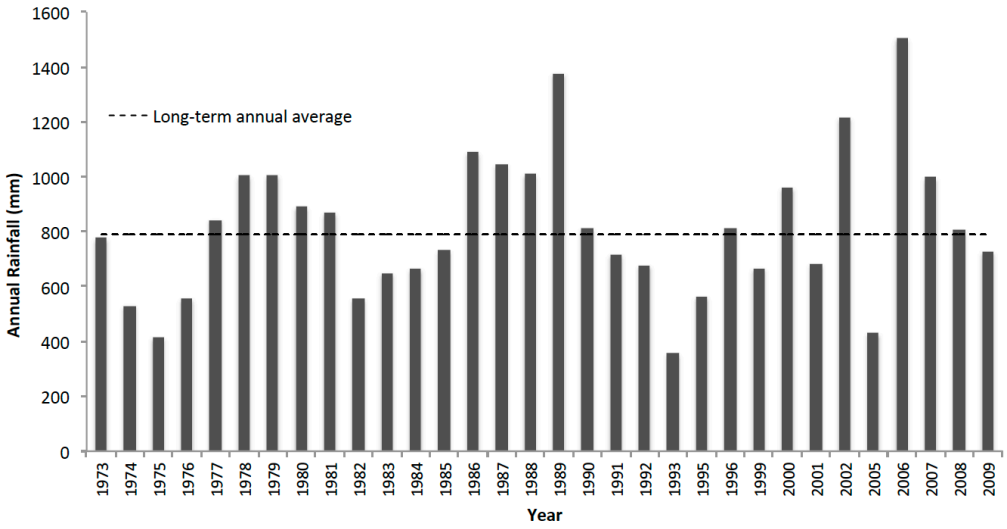

Figure 2. Annual Rainfall record at Babati station (1973–2009).

Hydrologically, the lake has no natural permanent surface outlet, but following a major flooding event (lake overflow) in 1964, a 4 m^3/s capacity artificial outlet connecting the lake to a gully system was constructed to prevent flooding of Babati town ([22,29]). Available lake level records are limited and erratic, covering two periods, i.e., 1978–1984, [25] and 2008–2012 (Internal Drainage Basin Water Office) (Figure 3). The records indicate an average lake depth of 5.27 m and 5.75 m for the first and second period respectively, with a standard deviation of 0.6 m for both periods. These correspond to 1–1.5 m less than the lake overflow level. The water level generally fluctuates about 1 m between the dry and wet season.

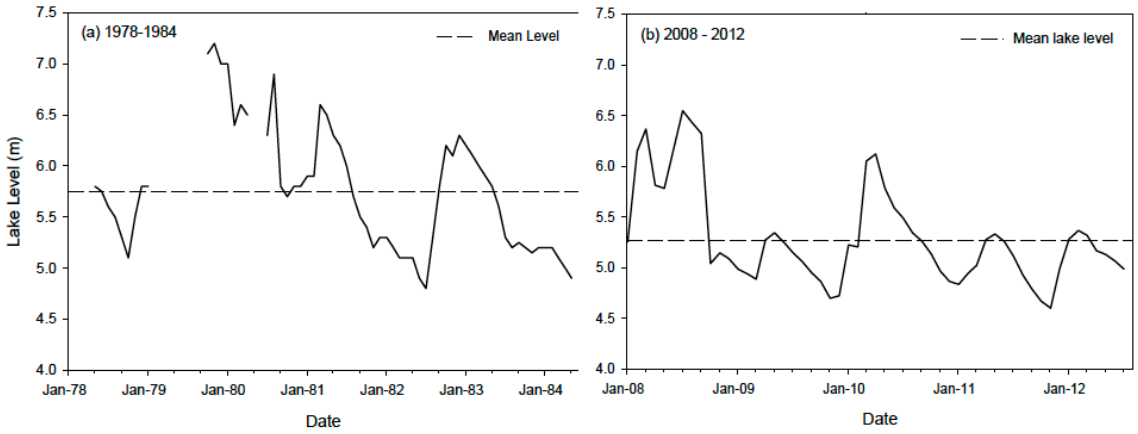

Figure 3. Lake level records for two different periods: (**a**) 1978–1984 and (**b**) 2008–2012.

The Lake Babati water balance is dominated by lake evaporation and runoff into the lake from the catchment area. Surficial runoff approximates 10% of the total catchment rainfall in the area [21] and can partly be a result of recent catchment deforestation [26,30]. Regional potential evapotranspiration rates near 1300 mm/year [28], but actual evapotranspiration is much lower due to limited available water through precipitation. High lake surface evaporation is a main cause of a positive net lake evaporation depth. Water exchange between the lake and the surrounding groundwater also plays an important role in lake level and salinity moderation. Observations indicate that lake overflow usually occurs some months after the rainfall maxima.

2.2. The Lake Water Balance Model

In this study, we consider a coupled lake-catchment model that consists of three modules: the lake, the adjacent groundwater reservoir and the remaining catchment area. The basis for the modelling is to maintain the water mass balance between input and output over the lake and its catchment area on an annual time step:

$$\frac{\Delta V_L + \Delta V_r}{\Delta t} = P(A_l + A_r + A_c) - E_l A_l - E_r A_r - E_c A_c - GW_f - R_f \quad (1)$$

where ΔV_L and ΔV_r are changes in lake and groundwater storage volumes (L^3) respectively; Δt the time step (T). We have assumed that the change of the groundwater volume in the upstream part of the catchment is equal to zero ($\Delta V_C = 0$). The reason is that ΔV_C is expected to be small relative to ΔV_L and ΔV_r, since the upstream part of the catchment is located further away from the lake, and will therefore be much less influenced by its (considerable) level variations. P is precipitation (L/T) estimated as being spatially uniform in this study for Lake Babati region from available rainfall records (Figure 2). A_l, A_r and A_c are the surface areas (L^2) of the lake, the groundwater reservoir adjacent to the lake, and the remaining upstream part of the catchment, respectively. These were determined from the lake bathymetry and catchment topography (Figure 4). E_l, E_r and E_c are the evaporation over the lake, the actual evapotranspiration over the groundwater reservoir adjacent to the lake and the actual evapotranspiration over the catchment (L/T), respectively. GW_f is the groundwater flux (L^3/T) draining out of the lake and R_f the possible runoff volume (L^3/T) due to lake overflow. These evaporative and water flux components were estimated as described in the following sections.

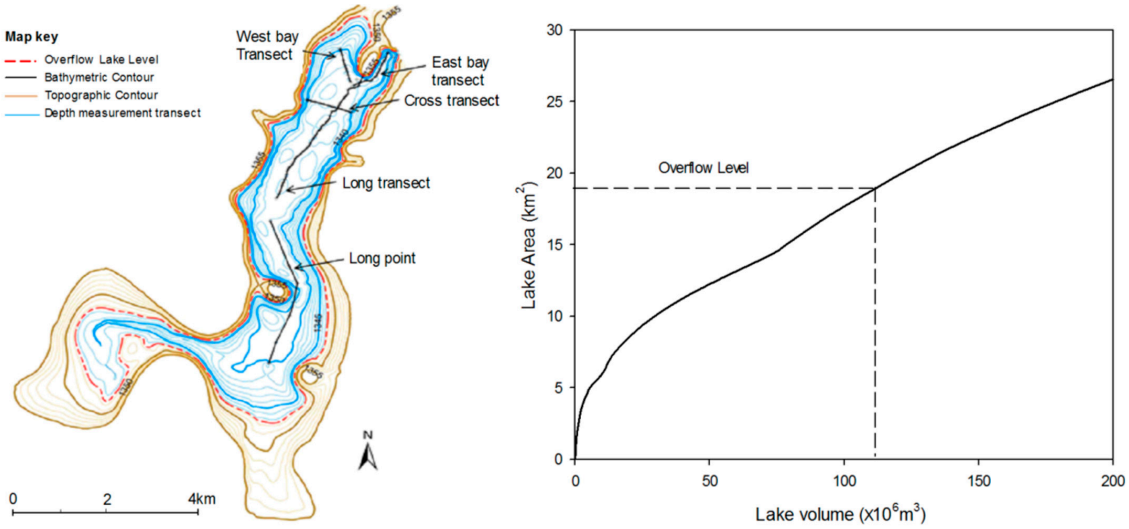

Figure 4. Lake Babati bathymetry (**left**) and area–volume relationship (**right**).

2.2.1. Catchment Topography and Lake Bathymetry

The area–volume relationship of the Lake Babati was derived from a combination of catchment topographic and lake bathymetric data (Figure 4). Catchment topography is based on a 90 m resolution Shuttle Radar Topography Mission (SRTM) digital elevation model (DEM) ([31]) and paper topographical maps (1:50,000 scale and 50 feet contour spacing) produced by the Directorate of Overseas Surveys for the Tanganyika Government in 1964 from aerial photographs taken in 1958–1960. The paper maps were georeferenced and important features (contours, river channels, lake shore, extent of alluvial deposits) were digitized. Hence, a topo-to-raster interpolation with drainage enforcement [32] within ArcGIS 10.1 spatial analyst package was applied to the digitized contours to generate a hydrologically correct 50 m resolution DEM, based on which (together with the SRTM DEM) the catchment boundary was delineated and its area calculated.

Subsequently, the contour line corresponding to the lake overflow level was used to determine the maximum lake surface area. Then, lake bathymetry was derived by spatial interpolation from lake vertical profile measurements along five transects acquired during a 2010 field visit (Figure 4). From the bathymetric map, the area and volume corresponding to different lake depths (from the lowest point to the maximum lake level, at 1 cm step) were calculated using the "surface volume" tool in ArcGIS 3D analyst. Finally, the area of the groundwater reservoir around the lake was determined based on the extent of the alluvial deposits as digitised from the topographic and geological maps.

2.2.2. Evaporation over the Lake

Lake surface evaporation is one of the main factors controlling the water balance of closed basin lakes. There are several methods to estimate lake surface evaporation, including direct measurements, empirical methods, water budget, energy budget, mass transfer and combination methods [33–36] or from pan evaporation records [37]. The Penman [35] and the energy balance methods have been extensively applied in the study of East African lakes [3–5].

In this study, the energy budget method was adopted. The approach is among the best methods for estimating open water evaporation [38–41]. Comparatively speaking, the energy budget method is relatively simple and less data intensive [42] and considers the effect of cloud cover, which is often ignored in other methods, despite its large impact on evaporation estimates. The approach is based on the assumption that, under steady-state conditions, the energy gained by the lake water surface from net radiation is compensated by the energy loss through latent and sensible heat transfer, such that:

$$R_n = H + H_L \tag{2}$$

where R_n is the net radiation (W/m^2), H is the sensible heat flux (W/m^2) and H_L the latent heat flux to evaporate water from the lake (W/m^2). In our case, it can be assumed that heat exchange between the lake surface and the deeper part of the lake is negligible, since the time step used (one year) is large enough to exclude the influence of diurnal cycles [33].

Equation (2) can be rewritten by introducing the Bowen ratio (B), which represents the fraction of sensible to the latent heat flux, as

$$B = H/H_L \tag{3}$$

$$H_L = \frac{R_n}{B+1} \tag{4}$$

The evaporation rate (E_L) can be introduced and represents the mass of water that needs to be evaporated to consume the latent heat energy of the latent heat and can be expressed as:

$$E_L = \frac{H_L}{L_e} = \frac{Rn}{(B+1)L_e} \tag{5}$$

where L_e is the latent heat of water vaporisation (2.46×10^6J/kg).

The net radiation (R_n) can be expressed in terms of the net short-wave radiation (R_s) and long-wave radiation (R_L) as:

$$R_n = R_S + R_L \tag{6}$$

Since there were no direct measurements, R_S and R_L were estimated in this study using empirical equations. The net shortwave radiation, which is the radiant flux resulting directly from solar radiation was estimated from [43] as:

$$R_s = (1-\alpha)R_{TOA}(0.803 - 0.34C - 0.458C^2) \tag{7}$$

α being the albedo of the water surface ($\alpha \approx 0.66$ [33]) and R_{TOA} is the solar radiation at the top of the atmosphere, which is a function of latitude [43]. R_{TOA} was estimated to be 416.4 W/m^2 at Lake Babati.

The parameter C, the cloud cover, explains the portion of the day during which clouds are not obstructing the sun. C values are highly variable and may have a great influence on lake evaporation estimates. It can be estimated from Equation (8) as:

$$C + \frac{n}{N} \cong 1 \tag{8}$$

where n and N are actual number of hours of bright sunshine and the number of daylight length, respectively [33]. The optimised value of C after model calibration was 0.4 (see following sections).

The net longwave radiation (R_L), the radiant flux resulting from emissions of the atmospheric gases and the land and water surfaces on earth, was estimated following [44] as:

$$R_L = \varepsilon_w \delta T_s^4 \left(0.39 - 0.05\sqrt{e_{sat}}\right)\left(1 - 0.53C^2\right) \tag{9}$$

where ε_w is the emissivity of water ($\varepsilon_w \approx 0.97$); δ is the Stephan–Boltzmann's constant ($\delta = 5.6697 \times 10^{-8}Wm^{-2} \cdot$K^{-4}), T_s is the lake surface temperature (K), and e_{sat} is the saturation vapor pressure (hPa), which can be calculated with Clausius–Clapeyron's relation as:

$$e_{sat} = 6.11\exp\left[\frac{\varepsilon L_e}{R_d}\left(\frac{1}{T_s} + \frac{1}{273.2}\right)\right] \quad (10)$$

where ε = 0.622 is the molar mass fraction of water vapour in dry air and R_d is the gas constant of dry air (287 J/kg/K).

The Bowen Ratio (B) is based on the eddy diffusivity hypothesis and is given by the relationship:

$$B = \frac{c_p}{L_e}\frac{T_r - T_s}{Q_r - Q_s} \quad (11)$$

where T_s and T_r are the temperature (K) at lake surface and at a reference height respectively. An average value of 19.4 °C (292.55 K) for the reference temperature was used. The lake surface water temperature was considered to vary with the air temperature (T_a) by a constant quantity ΔT, using the relation:

$$T_w = T_a + \Delta T \quad (12)$$

This simplification holds, since for such a shallow lake, a low heat storage value in the lake and thus a similar evolution of the air and water temperatures can be expected [4].

Q_r and Q_s are the specific humidity (%) at a reference height and close to the water surface respectively. The latter is approximated, assuming the near surface air temperature and the water surface temperature are the same and the relative humidity close to the surface is 100% (saturated air) using the relation:

$$Q_s = \frac{m_v}{m_v + m_d} \approx \frac{m_v}{m_d} = \frac{M_v}{M_d}\frac{e_{sat}}{p_o} = \varepsilon\frac{e_{sat}}{p_o} \quad (13)$$

where e_{sat} is the saturation vapour pressure (Pa) close to the water surface (Equation (10)); p_o is the atmospheric pressure at the lake surface, calculated by the relation:

$$p_o = p_{sea}\exp\left[-\left(\frac{g}{R}T_c\right)\Delta h\right] \quad (14)$$

where p_{sea} = 101,325 Pa is the sea level pressure, g = 9.81 m/s^2 is the acceleration of gravity, R = 287 is the gas constant of dry air, T_c is the average catchment temperature, and Δh is the altitude difference between the lake level and sea level. M_v and M_d are the molar masses of water vapour and dry air respectively (g/mol), assuming that the masses of the water vapor m_v and dry air m_d are such that $m_v \ll m_d$. The optimum value of 50% for relative humidity was determined from model calibration.

2.2.3. Evapotranspiration over the Groundwater Reservoir and the Catchment

Evapotranspiration over the ground is governed by several parameters including (but not necessarily limited to) the amount of water available in the surface layer, atmospheric conditions, the soil hydraulic conductivity of the soil, and plant type. Due to limited information about these variables in the study area, we used the empirical equations by [45,46] to estimate ground evapotranspiration. These relate evapotranspiration with precipitation and ground temperature as:

$$E_p = 325 + 21T_g + 0.9T_g^2 \quad (15)$$

$$E_a = \frac{P}{\sqrt{0.9 + \left(\frac{P}{E_p}\right)^2}} \quad (16)$$

where E_a and E_p are the actual and potential evapotranspiration rate respectively (kg/y/m^2 or mm/year), P the precipitation (mm/year), and T_g is average ground surface temperature (K). Since no measurements of catchment temperature were available, T_g was determined relative to the reference temperature at Babati town (1350 m a.s.l.), by assuming the standard atmosphere with a temperature increase of 0.6 K for every 100 m decrease in altitude. Therefore, E_r and E_c in the water balance

Equation (1) correspond to the actual evapotranspiration calculated at the mean altitude of the groundwater reservoir adjacent to the lake (1400 m a.s.l.) and at the mean altitude of the remaining upstream part of the catchment (1800 m a.s.l.) respectively, and adjusted by a calibration factor (X_c) to account for catchment dependency uncertainties [47], such that:

$$E_r = X_c E_a \tag{17}$$

with E_a calculated at 1400 m a.s.l. and

$$E_c = X_c E_a \tag{18}$$

with E_a calculated at 1800 m a.s.l.

The factor X_c was determined through calibration to be 1.15 (see Section 2.3).

2.2.4. Groundwater-Lake Water Interaction

Lake Babati water interaction with the surrounding groundwater reservoir also plays an important role in the water budget. The extent of the groundwater reservoir adjacent to the lake was determined from available topographical and geological information. The lake-groundwater interaction was modelled by assuming the change in groundwater storage depth (ΔD_r) equals the change in lake level (ΔD_l) from the net change in volume ($\sum \Delta V$) after each time step, such that:

$$\Delta D_r \cong \Delta D_l = \frac{\sum \Delta V}{A_L + A_r \varphi} \tag{19}$$

with φ being the mean porosity of the aquifer (-).

The groundwater flux leaving the lake (GW_f) was approximated by a Darcy flow, as

$$GW_f = -k_h A_{LW} s_g \tag{20}$$

where k_h is the aquifer horizontal hydraulic conductivity (m/s) and s_g the groundwater gradient (m/m), assumed equal to the topographical slope downstream of the lake. A_{LW} is the cross-sectional area perpendicular to the flow (m^2), expressed by the product of the water depth in the lake (D_L) and the average width of the downstream edge of the lake. Based on hydrogeological maps showing sandy aquifer conditions in the Lake Babati vicinity [48], the hydraulic conductivity (k_h) and porosity (φ) were set accordingly [49,50] to 50 m/day and 40% respectively.

2.3. Model Structure, Input Parameters, Calibration, and Sensitivity

A Fortran-based program was developed to solve the mass balance (Equation (1)) following the calculation workflow in Figure 5. The program first calculates the net water volume change from the combined input (precipitation) and output (evaporation and groundwater leakage) fluxes at the end of a time step (1 year). Then, based on the area–volume relationship, the corresponding lake level change (positive or negative) is determined and used to update the lake level from the previous time step. The procedure is repeated iteratively starting from an initial lake water depth taken from observations until the lake level change between two successive iterations is small enough (<10 mm/year) or the lake has dried out completely. Upon convergence of a solution, the evolution of different water balance components over the simulation period is recorded in a text file for further analysis. The choice of the annual time step was motivated by data availability. Moreover, the annual time step was adequate since the study sought to establish the annual water balance of the lake-catchment system and assess the sensitivity to changes in long-term hydroclimatic conditions, rather than on seasonal dynamics such as in [3,51].

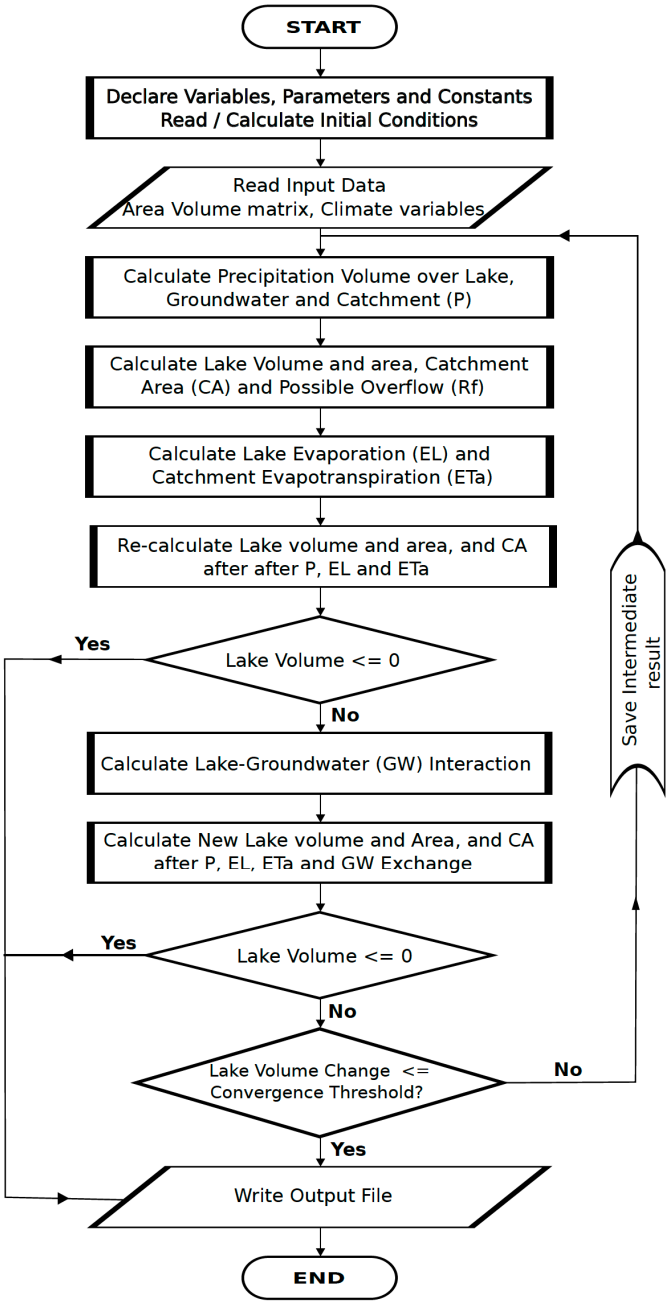

Figure 5. Workflow of the water balance model calculation.

Model parameters (Table 1) were, to a large extent, independently derived from available meteorological, hydrogeological and lake level records, as described in previous sections. However, there were no site-specific data on the cloud cover fraction (C) and the factor X_c for adjusting actual evapotranspiration Equations (17) and (18). Thus, these were determined through calibration, constraining them within physically reasonable parameter ranges derived from parallel studies. From sunshine duration estimates in this world region [28], cloud cover can be expected to be between 0.3 and 0.5. Furthermore, from analyses of different hydroclimatic regions (including tropical, temperate and arid conditions), X_c has been found to range between 0.7 and 1.2 [12,47,52–54]. This reflects an error in the estimated evapotranspiration on the order of 20% to 30%, which e.g., is lower than errors of about 50% that were reported in a synthesis of [52]. A possible reason for the relatively

low errors is that these studies consider annual or multi-annual averages over catchments, as opposed to short-term, point values which are considerably more difficult to predict.

Table 1. Summary of model input variables, physically plausible range of parameters used in the calibration, and resulting optimum parameter value after calibration to observations.

Model Input	Estimated Current Value	
Precipitation (mm/year)	789.0	
Temperature (°C)	19.4	
Relative Humidity (%)	50.0	
Lake surface area (km^2)	6.9	
GW reservoir area (km^2)	48.1	
Total catchment area (km^2)	355.0	
Groundwater conductivity (m/day)	50.0	
Porosity (%)	40.0	
Calibrated parameters	Physical range	Optimum value
Cloud Cover (C) (%)	0.3–0.5	0.40
Calibration factor for ET (X_c)	0.7–1.2	1.15

Considering these bounds (Table 1), the model was run in steady state with several pairs of the two parameters (C, X_c) over the period 1978–1984, resulting in a response surface map (Figure 6) showing the evolution of the deviation between observed and simulated lake level. The parameter combination that gave the least deviation between observed and modelled lake levels during the calibration period was determined as C = 0.4 and X_c = 1.15. A factor contributing to the relatively good closure (i.e., X_c is close to unity) can be that, despite the previously mentioned large inter-annual variations, the average precipitation and other ambient conditions are shared with relatively many other regions of the world, which means that the empirical basis for the used model coefficients is good.

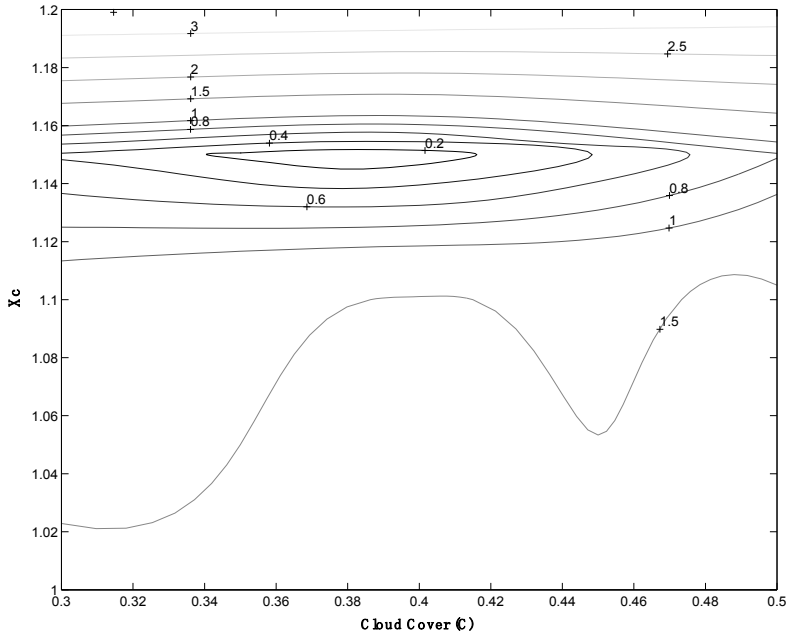

Figure 6. Model Response Map for calibration of cloud cover C and factor X_c (contour levels represent deviation between simulated and observed lake water level).

The ability of the model, calibrated to current conditions according to the above description, to reproduce available historical lake level variations was tested through simulation of lake level dynamics based on observed annual precipitation for the period 1978–1984. The inter-annual lake

level variation was well reproduced with an average deviation from observed lake level of 8%. This is adequate, considering that variations in other variables (e.g., temperature) were not taken into account during simulation.

Moreover, since available historical data on average lake levels (covering 10 years; 1978 to 1984 and 2008 to 2011) did not overlap sufficiently with available data on average annual precipitation (covering the years 1973 to 2009), we investigated if the model, given a 50-year synthetic p data series with the same mean and standard deviation as the observed one (789 $\pm$ 278 mm/year), was able to yield lake levels that were consistent with the observed levels in terms of mean value and standard deviation. To ensure the synthetic time series is consistent with the observed series, we first performed normality and autocorrelation tests on the historical P dataset. Following the Weibull method [55], the observed p dataset was normally distributed with both its probability density function (PDF) and cumulative density function (CDF) within a 95% confidence range. Moreover, there was no significant autocorrelation within the dataset. Therefore, we assumed a Gaussian distribution, with zero autocorrelation to generate the synthetic time series.

Since estimates of the true standard deviation from only ten samples (historical lake level observations) are associated with uncertainty, we calculated a 95% confidence interval for this true standard deviation according to:

$$\sqrt{\frac{(n-1)\,\sigma^2}{\chi^2_{right}}} < \sigma < \sqrt{\frac{(n-1)\,\sigma^2}{\chi^2_{left}}} \tag{21}$$

where n is the sample size, σ is the sample standard deviation, and χ^2_{right} and χ^2_{left} are the right side and left side chi-square standard values for $n-1$ degrees of freedom. The performance of the model with respect to reproducing historical data was evaluated from the agreement between the mean lake level of the historical observations and the simulated one, as well as the consistency between the simulated lake level variation and the true value (checking if the simulated level variations fall within the confidence interval for the true level variations). We note that this test is based on an implicit assumption that precipitation variability is a main driver of lake level variation—this hypothesis was tested separately through sensitivity analysis.

A sensitivity analysis was performed in order to determine the influence of four important hydroclimatic parameters (precipitation, temperature, cloud cover and relative humidity) to the lake level and the lake evaporation. This sensitivity analysis involved varying one parameter at a time over a certain range of values and observing the resulting change in lake level and lake evaporation. Precipitation and air temperature were varied at regular intervals over a range of values to drive the lake level from dry-out to overflow conditions. Cloud cover and relative humidity were varied over their full range of possible values (0%–100%).

2.4. Assessment of Future Climatic Conditions

In order to assess the lake response to future climatic changes, ensemble means of projected future temperature and precipitation changes from four Representative Concentration Pathways (RCPs) of the Coupled Model Intercomparison Project, Phase 5 (CMIP5) [56] were used to force the calibrated model from current conditions. The data were retrieved from the Royal Netherlands Meteorological Institute (KNMI) Climate Change Atlas [57]. Accordingly, over the 21st century, the study area is expected to experience a temperature rise of between 0.75 to 3.5 °C and an increase in average annual precipitation of around 5% to 10% (Table 2). When using these future projections, simulations were run for the mean future changes as well as for the means plus/minus one standard deviation, to have an idea on possible variability. During simulation, the total projected changes were linearly distributed over a 100-year period, while keeping model parameters fixed at their present day calibrated values.

Table 2. Projected future climate change at Lake Babati based on CMIP5 ensemble mean (2080–2100). The values in brackets represent the standard deviation.

Climate Variable	RCP2.6	RCP4.5	RCP6.0	RCP8.5
Temperature Change (°C)	+0.75 (0.6)	+2 (0.1)	+2.5 (0.4)	+3.5 (0.5)
Precipitation Change (%)	+5 (21)	+10 (16)	+10 (27)	+10 (33)

3. Results and Discussion

3.1. Reproducing Current Conditions and Historical Observations at Lake Babati

The estimated lake and its catchment water balance components are presented in Table 3. The simulated average water level is 5.32 m, that is 50 mm (1%) higher than the observed average level (5.27 m) between 2008 and 2012. Surface evaporation from the lake amounts to 1.44×10^7 m^3 (2075.7 mm/year), i.e., more than twice the precipitation volume of 5.331×10^6 (789 mm/year), thus represents an important part of the water budget over the lake.

Table 3. Model estimated components of Lake Babati water balance (2008–2012).

Component/Term	Value
Lake depth (m)	5.32
Lake volume (m^3)	1.391×10^7
Precipitation over the lake (m^3/year)	5.331×10^6
Precipitation over ground (m^3/year)	2.679×10^8
Lake Evaporation (m^3/year)	1.437×10^7
Actual ET over ground (m^3/year)	2.552×10^8
Groundwater Leakage (m^3/year)	3.671×10^6
Lake overflow volume (m^3/year)	0
Discrepancy (as % of Lake Volume)	<1%
Net lake evaporation depth (mm/year)	1286
Lake inflow factor (-)	0.7

This is typical of many East African and tropical lakes, such as Lake Manyara [6], Lake Nakuru [58], Lake Ziway [4], and many others [59,60]. The total precipitation volume over the whole catchment (including the lake) is 2.72×10^8 m^3/year which is however far greater (almost 20 times) than the lake surface evaporation volume (1.44×10^7 m^3/year).

The current groundwater flux from the lake is estimated to be 3.67×10^6 m^3/year representing about 26% of the average lake volume. The actual evapotranspiration loss over the catchment (excluding the lake) is 2.55×10^8 m^3/year, which is approximately 93% of the total catchment precipitation. This is consistent with an earlier suggestion by [21], who reported a catchment runoff coefficient between 2% and 10% for the study area. The net lake evaporation depth (the difference between evaporation and precipitation depth over the lake) is 1286 mm/year while the lake inflow factor (i.e., the ratio of surface and groundwater inflow volume into the lake to the total input volume to the lake by surface inflow, groundwater flow, and direct precipitation) is 0.7. The latter is comparable to those of other East African terminal lakes, including Lake Manyara (0.5) [6], Lake Naivasha (0.7), Lake Awassa (0.5) and Lake Shala (0.7) [61].

Considering historical conditions, the simulated average lake level was 5.05 m, with a standard deviation of 0.9 m (Figure 7). This value corresponds to 4% less than the observed lake level (5.27 m). Furthermore, we calculated the 95% confidence interval for the true standard deviation of the historical lake level to range from 0.41 to 1.09 m (i.e., an observed standard deviation around 0.7 m). Hence, the simulated standard deviation of 0.9 m falls within this confidence range. Although this suggests about a 30% bias in temporal variability of lake level, we consider that the model can reproduce fairly well the variations of the past in terms of lake volume.

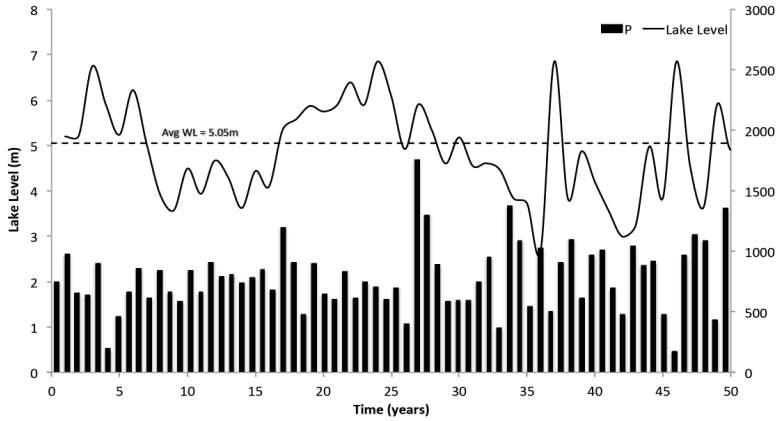

Figure 7. Simulation of Lake Babati level variation based on a 50-year random precipitation time series generated using historical mean and standard deviation values of precipitation for the period 1973 to 2009.

3.2. *Sensitivity Analysis*

The lake level sensitivity to changes in precipitation, temperature, cloud cover and relative humidity are presented in Figure 8. The horizontal dashed lines represent the current lake level and the vertical dashed lines correspond to the current value (present conditions) of the respective parameter. It is observed that precipitation change has a relatively large impact on lake level (Figure 8a). For example, an increase of about 10% (90 mm/year) in annual average precipitation would lead to lake overflow (1.5 m rise), while a 17% (140 mm/year) decrease in rainfall results in dry-out conditions (5.3 m drop). In contrast to this, temperature changes inversely affect lake levels (Figure 8b) with a 2.4 °C temperature decrease from present conditions resulting in lake overflow while a 3.6 °C increase leads to lake dry out.

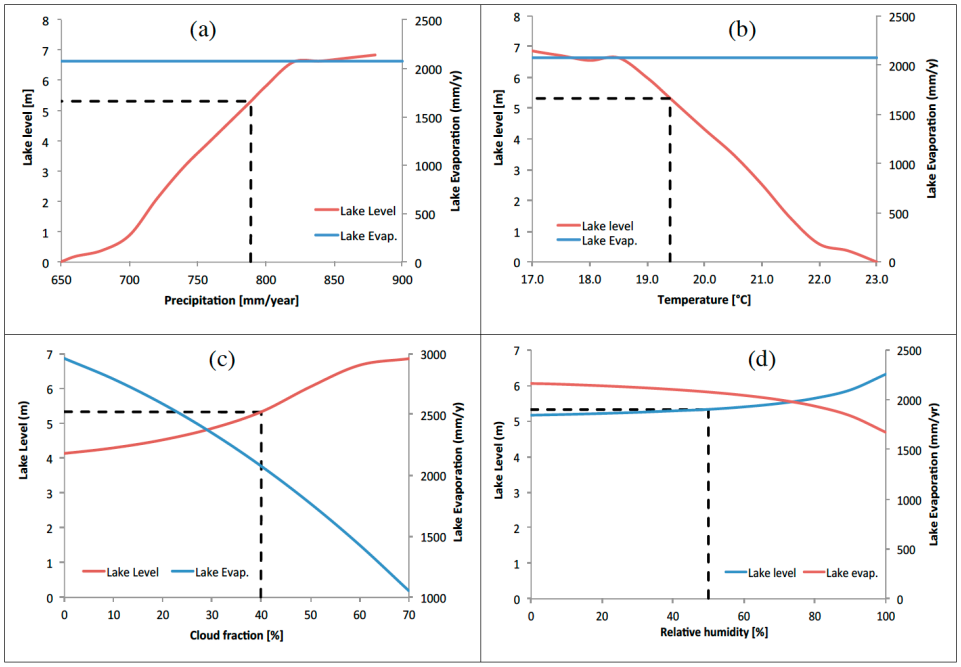

Figure 8. Lake water level sensitivity to changes in (**a**) Precipitation; (**b**) Temperature; (**c**) Cloud Fraction and (**d**) Relative Humidity. The horizontal dashed line represents the current lake level and the vertical dashed line corresponds to the current value of the respective parameter.

Lake levels are also relatively sensitive to changes in cloud cover fraction (Figure 8c). A 30% increase in cloud cover fraction from present conditions results in lake overflow, however, complete dry-out could not be obtained even if the cloud cover fraction were to be reduced to its lowest value (0%). Apparently, there is no appreciable response in lake level when the cloud cover drops below 20%. Another important observation is the significant impact of cloud cover fraction on lake evaporation. Changing the cloud cover from 0% to 70% would cause lake evaporation to drop substantially by about 2000 mm/year, i.e., about 285 mm/year for every 10% change in cloud cover. Changing relative humidity (Figure 8d) seems to have little effect on lake levels; varying relative humidity from 0% to 100% results in only a 1 m water rise. The effect of relative humidity on lake evaporation is also less pronounced and mainly occurs above 50%. Over the full range of relative humidity (0%–100%), the change in lake evaporation is about 400 mm/year. This corresponds to an average reduction of 40 mm/year in lake evaporation for every 10% decrease in relative humidity. The magnitude of change in each of the four parameters required for bringing the lake level from dry-out to overflow conditions are summarised in Table 4.

Table 4. Changes in parameter leading to overflow or dry-out from the present lake level.

Lake Level Change	Temperature (°C)	Precipitation (mm/Year)	Cloud Cover (%)	Relative Humidity (%)
Current to Overflow	−2.4	+90	+30	did not occur
Current to Dry-out	+3.6	−140	did not occur	did not occur
Dry-out to overflow (absolute)	6	230	n/a	n/a

Note: n/a stands for "not applicable".

The sensitivity analysis results indicate that the lake is highly sensitive to changes in precipitation, and relatively sensitive to air temperature and cloud cover fraction, while less sensitive to changes in relative humidity (Figure 8). Our results support those of [60], who studied the sensitivity of 10 East African lakes to climate fluctuations. They associated high lake level sensitivity not only to the size and morphology of the lakes, but also to higher values of the aridity index, a factor which directly reflects precipitation and evaporation contribution [62]. Likewise, high sensitivity to changes in precipitation has been observed at Lake Suguta, Kenya [8]. The exceptional low sensitivity to precipitation at Lake Tana has been associated with its relatively significant outflow [5].

High sensitivity to temperature has been reported for Lake Ziway, Ethiopia [4], and Lake Victoria [3,11] whereas the impact of cloud cover on the level of East African lakes seems not to have been reported before; its relatively high impact on lake evaporation has also been seen for Lake Victoria, where lake evaporation was reduced by 252 mm per year (15%) when cloud cover increased by 7%. Similar findings are reported for the Nakuru-Elmenteita lake basin, Kenya, where a 10% increase in cloudiness resulted in a 5.5% reduction of lake evaporation [58]. A methodologically similar study to ours was conducted by [63], who investigated the impact of sunshine index (a proxy of cloudiness) on the level of Lake Bosumtwi, Ghana (West Africa), showing as in the present case, a large impact. Finally, the relative humidity was found to have nearly no effect at Lake Ziway [4].

Considering that available precipitation and temperature data are often less uncertain than cloudiness data due to more frequent and direct measurement, our results emphasise the importance of considering the cloudiness as a crucial factor in estimating lake surface evaporation. This aspect has often been overlooked in most lake-catchment modelling studies in the region. However, it is important to note that the lake sensitivity results presented above are influenced by the calculation methods and assumptions made. For example, lake evaporation was calculated by the energy balance method, whose sensitivity to air temperature is relatively higher than in the Penman method [3]. Similarly, evaporation is slightly more sensitive to relative humidity changes in the Penman method than it is in the energy balance equation or the Complementary Relationship Lake Evaporation (CRLE) model [4]. Besides, as also observed by [60], lake size and morphology plays an important role in lake sensitivity to climatic forcing.

3.3. Lake Babati Response to Climate Change and Variability

The solid lines of Figure 9 show the lake response to the ensemble mean projection of changes in temperature and precipitation over the 21st century, for different climate forcing scenarios (green—RCP2.6: cyan—RCP4.5; blue—RCP6.0; red—RCP8.5). Two distinct lake evolution patterns can be observed, depending on the relative importance of the opposite effects of temperature and precipitation. The first pattern brought about by the RCP6.0 scenario (+2.5 °C, +10%P) and RCP8.5 (+3.5 °C, +10%P) indicates that the current lake level will drop by 1.6 m and 3.4 m, respectively, at the end of the century. Volumetrically, this corresponds to 61% and 93% reductions at the end of the century. Such depletion would directly impact the water supply availability for Babati town and would have serious implications on the sustainability of the lake aquatic ecosystem (e.g., hippos, fish and birds).

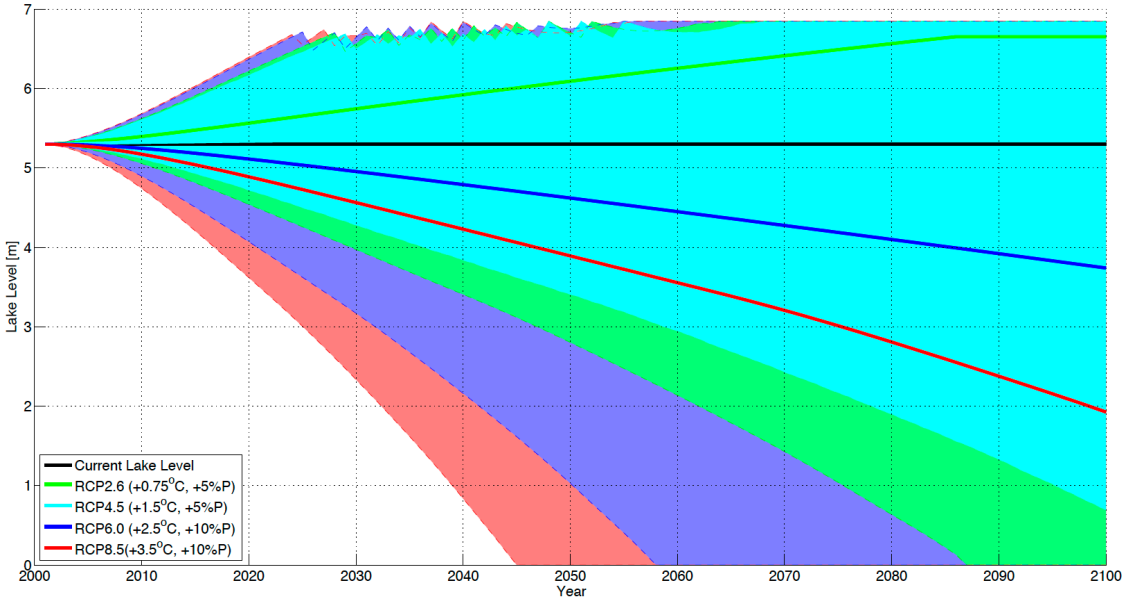

Figure 9. Lake Babati response to climate change scenarios. The thick solid lines represent lake response to ensemble mean change in precipitation and temperature; the shaded areas represent the one standard deviation confidence range for each scenario; bounded with thin dashed lines of the same color as the mean response lines.

The second pattern brought about from the RCP2.6 scenario (+0.75 °C, +5%P) consists of a gradual water level rise, leading to lake overflow level after about 80 years. This would be positive in terms of water availability and aquatic ecosystem support, however, it would reduce considerably the lake's flood buffering capability and, thus, increase Babati town vulnerability to flooding. The RCP4.5 scenario (+1.5 °C, +5%P) does not seem to affect the lake level significantly.

Although the above discussed ensemble mean projections generally have better predictive capacity in hydrological and lake balance applications than individual model results ([12,53]), an important observation is that output from individual climate models in the present case yield large differences in predicted lake response. More specifically, the shaded area bordered by dashed lines in Figure 9 indicates simulation results for the ensemble mean temperature and precipitation plus/minus one standard deviation. The funnel-like shape of all shaded areas in Figure 9 suggests that for any of the four climate forcing scenarios, Lake Babati could reach overflow conditions in as soon as twenty years. On the other hand, with the exception of the RCP4.5 scenario, the lake could potentially dry out [about 45 years (RCP8.5), 60 years (RCP6.0), and 90 years (RCP2.6)]. This high variability in lake response can be explained by the high variability in precipitation predictions within individual climate model projections. The standard deviation of the projected precipitation increase ranged between

26% and 33% (Table 2). According to sensitivity results (Section 3.2), this is comparable to the amount of precipitation change that could drive the lake from dry-out to overflow conditions. On the other hand, the maximum standard deviation in projected temperature change across the four scenarios is 0.6 °C, which is only 10% of the total warming or cooling required to move the system from overflow to dry-out.

Our results emphasize that the high uncertainty in the ability of individual global climate models (GCMs) to project future rainfall changes in the tropics may result in high uncertainty in both magnitude and direction of the simulated hydrological responses of highly sensitive systems. This amplifies the vulnerability in Lake Babati owing to the lake's high sensitivity to slight changes in precipitation and makes it difficult to project robust future lake level estimates independent of the future emission scenario considered. While it is this sensitivity that has likely brought about the limited attempts to quantify actual impacts of future climate change, as projected by GCMs, on lakes response in East Africa, there is still a need to consider lake evolution through various scenarios as such investigations can potentially inform management options. For instance, ensemble mean projection results that are known to have better predictive than individual models results suggest in the present case that a future temperature increase by 2 °C or more increases the risk of complete lake dry-out. Managing the profound effect on regional water resources of such a development is associated with considerable challenges that most likely would need to be identified well in time in order to reach viable and efficient solutions. Future work coupling groundwater and lake interactions that allows characterization of, for example, spatiotemporal variability of landscape responses (e.g., [64]) thereby isolating sub-annual fluxes and process shifts could help isolate impacts of the largest GCM uncertainties. Further, utilization of downscaled modelling output or regional models may help refine the large uncertainties in future projections. Lastly, it should be noted that the validity of analysis above might be influenced by a number of other factors in addition to the GCM uncertainty which were not explicitly considered in the model. For example, future shifts in cloud cover fraction will affect lake evaporation and alter the lake response. Also, land cover changes could alter surface runoff (e.g., [65]), sedimentation, groundwater discharge, lake storage and buffering, eventually attenuating or aggravating the climate change impacts.

4. Conclusions

Based on region and site specific hydrogeological and hydro-climatic input, a novel coupled approach that accounts for lake water-groundwater interactions could reproduce existing observations on current and historic lake levels of the semi-closed freshwater Lake Babati in Tanzania (East Africa). Results on lake level sensitivity to cloudiness (cloud cover), which seems not to have been assessed for East African lake systems before, show that cloudiness is a main parameter affecting lake levels together with precipitation and temperature. Increased focus on cloud cover measurement and interpretation could likely improve projections of lake levels and surface water availability, since cloudiness generally is subject to less frequent and direct measurements than precipitation and temperature. Precipitation change had a relatively large impact on lake levels as seen previously in other studies. We conclude more specifically that the divergent results on the future (21st century) development of Lake Babati can be explained by the fact that the variability in precipitation output of individual CMIP5 global climate models is comparable to the amount of precipitation change that is needed to drive the model from lake dry-out to overflow; this condition is likely shared with many other East African lake systems. Relatively dependable ensemble mean projection results show that a future temperature increase by 2 °C or more increases the risk of complete lake dry-out. Managing the profound effect on regional water resources of such a development is associated with considerable challenges that most likely would need to be identified well in time in order to reach viable and efficient solutions. More generally, present results highlight key change-driving processes and factors in the complex dynamics relating lake systems response to future climatic changes, indicating that it could be useful

to apply the methodology to study other water bodies in data-scarce areas of tropical Africa, in order to support sustainable water resource planning and management.

Acknowledgments: The authors acknowledge financial support from the Swedish International Development Agency (Sida) Project Number SWE-2011-066 and Sida Decision 2015-000032 Contribution 51170071 Sub-project 2239.

Author Contributions: René P. Mbanguka and Jerker Jarsjö conceived and designed the study, René P. Mbanguka performed simulations, analysed the data and wrote majority of the manuscript, Jerker Jarsjö and Steve W. Lyon contributed analysis and write-up, Marc Girons Lopez provided initial modelling codes, and Karin Holmgren contributed to write up.

Conflicts of Interest: The authors declare no conflict of interest.

References

1. Swenson, S.; Wahr, J. Monitoring the water balance of Lake Victoria, East Africa, from space. *J. Hydrol.* **2009**, *370*, 163–176. [CrossRef]
2. Tate, E.; Sutcliffe, J.; Conway, D.; Farquharson, F. Water balance of Lake Victoria: Update to 2000 and climate change modelling to 2100. *Hydrol. Sci. J.* **2004**, *49*. [CrossRef]
3. Yin, X.G.; Nicholson, S.E. The water balance of Lake Victoria. *Hydrol. Sci. J.* **1998**, *43*, 789–811. [CrossRef]
4. Vallet-Coulomb, C.; Legesse, D.; Gasse, F.; Travi, Y.; Chernet, T. Lake evaporation estimates in tropical Africa (Lake Ziway, Ethiopia). *J. Hydrol.* **2001**, *245*, 1–18. [CrossRef]
5. Kebede, S.; Travi, Y.; Alemayehu, T.; Marc, V. Water balance of Lake Tana and its sensitivity to fluctuations in rainfall, Blue Nile Basin, Ethiopia. *J. Hydrol.* **2006**, *316*, 233–247. [CrossRef]
6. Deus, D.; Gloaguen, R.; Krause, P. Water balance modeling in a semi-arid environment with limited in situ data using remote sensing in Lake Manyara, East African Rift, Tanzania. *Remote Sens.* **2013**, *5*, 1651–1680. [CrossRef]
7. Bergner, A.G.N.; Trauth, M.H.; Bookhagen, B. Paleoprecipitation estimates for the Lake Naivasha basin (Kenya) during the last 175 k.y. using a lake-balance model. *Glob. Planet. Chang.* **2003**, *36*, 117–136. [CrossRef]
8. Borchardt, S.; Trauth, M.H. Remotely-sensed evapotranspiration estimates for an improved hydrological modeling of the early Holocene mega-lake Suguta, northern Kenya Rift. *Palaeogeogr. Palaeoclimatol. Palaeoecol.* **2012**, *361–362*, 14–20. [CrossRef]
9. Legesse, D.; Vallet-Coulomb, C.; Gasse, F. Analysis of the hydrological response of a tropical terminal lake, Lake Abiyata (Main Ethiopian Rift Valley) to changes in climate and human activities. *Hydrol. Process.* **2004**, *18*, 487–504. [CrossRef]
10. Koutsouris, A.J.; Destouni, G.; Jarsjö, J.; Lyon, S.W. Hydro-climatic trends and water resource management implications based on multi-scale data for the Lake Victoria region, Kenya. *Environ. Res. Lett.* **2010**, *5*. [CrossRef]
11. Yin, X.; Nicholson, S.E.; Ba, M.B. On the diurnal cycle of cloudiness over Lake Victoria and its influence on evaporation from the lake. *Hydrol. Sci. J.* **2000**, *45*, 407–424. [CrossRef]
12. Jarsjö, J.; Asokan, S.M.; Prieto, C.; Bring, A.; Destouni, G. Hydrological responses to climate change conditioned by historic alterations of land-use and water-use. *Hydrol. Earth Syst. Sci.* **2012**, *16*, 1335–1347. [CrossRef]
13. National Bureau of Statistics (NBS). *2012 Population and Household Census. Population Distribution by Administrative Areas*; National Bureau of Statistics and Office of Chief Government Statistician: Dar es Salaam and Zanzibar, Tanzania, 2013; p. 264.
14. Kahurananga, J. *Lake Babati, Tanzania and Its Immediate Surroundings. Part I—Baseline Information*; Regional Soil Conservation Unit (SIDA): Nairobi, Kenya, 1992.
15. Strömquist, L.; Johansson, D. Studies of soil erosion and sediment transport in the Mtera reservoir region, Central Tanzania. *Z. Geomorphol.* **1978**, *29*, 43–51.
16. Muzuka, A.N.N.; Ryner, M.; Holmgren, K. 12,000-year, preliminary results of the stable nitrogen and carbon isotope record from the Empakai Crater lake sediments, Northern Tanzania. *J. Afr. Earth Sci.* **2004**, *40*, 293–303. [CrossRef]

17. Öberg, H.; Norström, E.; Malmström Ryner, M.; Holmgren, K.; Westerberg, L.O.; Risberg, J.; Eddudóttir, S.D.; Andersen, T.J.; Muzuka, A. Environmental variability in northern Tanzania from ad 1000 to 1800, as inferred from diatoms and pollen in Lake Duluti. *Palaeogeogr. Palaeoclimatol. Palaeoecol.* **2013**, *374*, 230–241. [CrossRef]
18. Ryner, M.; Holmgren, K.; Taylor, D. A record of vegetation dynamics and lake level changes from Lake Emakat, northern Tanzania, during the last c. 1200 years. *J. Paleolimnol.* **2008**, *40*, 583–601. [CrossRef]
19. Ryner, M.A.; Bonnefille, R.; Holmgren, K.; Muzuka, A. Vegetation changes in Empakaai Crater, northern Tanzania, at 14,800–9300 cal·yr BP. *Rev. Palaeobot. Palynol.* **2006**, *140*, 163–174. [CrossRef]
20. Strömquist, L.; Johansson, D. *An Assessment of Environmental Change and Recent Lake Babati Floods, Babati District, Tanzania*; LandFocus Consultants: Uppsala, Sweden, 1990.
21. Sandström, K. The recent lake babati floods in semi-arid Tanzania—A response to changes in land cover? *Geogr. Ann.* **1995**, *77 A*, 35–44. [CrossRef]
22. Gerdén, C.Å.; Khawange, G.M.O.; Mallya, J.M.; Mbuya, J.P.; Sanga, R.C. The Wild Lake. In *The 1990 Floods in Babati, Tanzania—Rehabilitation and Prevention*; Regional Soil Conservation Unit (SIDA): Nairobi, Kenya, 1992.
23. Andrews, P.; Bamford, M.K.; Njau, E.F.; Leliyo, G. The ecology and biogeography of the endulen-laetoli area in northern Tanzania. In *Paleontology and Geology of Laetoli: Human Evolution in Context*; Harrison, T., Ed.; Springer: Dordrecht, The Netherlands, 2011; pp. 167–200.
24. Koponen, J. Structures, people and production in Late Pre-Colonial Tanzania: History and structures. *J. Afr. Hist.* **1991**, *32*, 155–156.
25. Strömquist, L. Environmental impact assessment of natural disasters, a case study of the recent Lake Babati floods in northern Tanzania. *Geogr. Ann. Ser. A Phys. Geogr.* **1992**, *74*, 81–91. [CrossRef]
26. Newman, P.; Rönnberg, P. *Changes in Land Utilization within the Last Three Decades in the Babati Area*; International Rural Development Centre, Swedish University of Agricultural Sciences: Uppsala, Sweden, 1992.
27. Kijazi, A.L.; Reason, C.J.C. Analysis of the 2006 floods over northern Tanzania. *Int. J. Climatol.* **2009**, *29*, 955–970. [CrossRef]
28. Food and Agriculture Organization of the United Nations (FAO). *New_Locclim: Local Climate Estimator Version 1.10*; Environment and Natural Resources Working Paper No. 20 (CD-ROM); FAO: Rome, Italy, 2005.
29. Sjödin, E. *Leaking or Waterproof Organization? Babati Town and the Current Capacity to Handle Floods*; Södertörn Högskola: Huddinge, Sweden, 2010.
30. Yanda, P.Z.; Madulu, N.F. Water resource management and biodiversity conservation in the Eastern Rift Valley Lakes, northern Tanzania. *Phys. Chem. Earth* **2005**, *30*, 717–725. [CrossRef]
31. Jarvis, A.; Reuter, H.I.; Nelson, A.; Guevara, E. Hole-Filled Seamless SRTM Data V4. International Center for Tropical Agriculture (CIAT). 2008. Available online: http://srtm.csi.cgiar.org (accessed on 17 September 2015).
32. Hutchinson, M.F. A new procedure for gridding elevation and stream line data with automatic removal of spurious pits. *J. Hydrol.* **1989**, *106*, 211–232. [CrossRef]
33. Brutsaert, W. *Evaporation into the Atmosphere: Theory, History, and Applications*; Reidel: Dordrecht, The Netherlands, 1982; p. 299.
34. Morton, F.I. Practical estimates of lake evaporation. *J. Clim. Appl. Meteorol.* **1986**, *25*, 371–387. [CrossRef]
35. Penman, H.L. Natural evaporation from open water, bare soil and grass. *Proc. R. Soc. Lond. Ser. A Math. Phys. Sci.* **1948**, *193*, 120–145. [CrossRef]
36. Singh, V.P.; Xu, C.Y. Evaluation and generalization of 13 mass-transfer equations for determining free water evaporation. *Hydrol. Process.* **1997**, *11*, 311–323. [CrossRef]
37. Kummu, M.; Tes, S.; Yin, S.; Adamson, P.; Józsa, J.; Koponen, J.; Richey, J.; Sarkkula, J. Water balance analysis for the tonle sap lake-floodplain system. *Hydrol. Process.* **2014**, *28*, 1722–1733. [CrossRef]
38. Kutzbach, J.E. Estimates of past climate at Paleolake Chad, North Africa, based on a hydrological and energy-balance model. *Quat. Res.* **1980**, *14*, 210–223. [CrossRef]
39. Lenters, J.D.; Kratz, T.K.; Bowser, C.J. Effects of climate variability on lake evaporation: Results from a long-term energy budget study of Sparkling Lake, northern Wisconsin (USA). *J. Hydrol.* **2005**, *308*, 168–195. [CrossRef]

40. Rosenberry, D.O.; Sturrock, A.M.; Winter, T.C. Evaluation of the energy budget method of determining evaporation at Williams Lake, Minnesota, using alternative instrumentation and study approaches. *Water Resour. Res.* **1993**, *29*, 2473–2483. [CrossRef]
41. Winter, T.C. Uncertainties in estimating the water balance of lakes. *JAWRA J. Am. Water Resour. Assoc.* **1981**, *17*, 82–115. [CrossRef]
42. Hastenrath, S.; Kutzbach, J.E. Paleoclimatic estimates from water and energy budgets of East African lakes. *Quat. Res.* **1983**, *19*, 141–153. [CrossRef]
43. Black, J.N.; Bonython, C.W.; Prescott, J.A. Solar radiation and the duration of sunshine. *Q. J. R. Meteorol. Soc.* **1954**, *80*, 231–235. [CrossRef]
44. Budyko, M.I. *Climate and Life*; Academic Press: New York, NY, USA, 1974.
45. Langbein, W.B. Annual runoff in the United States. *Geol. Surv. Circ.* **1949**, *52*, 14.
46. Turc, L. The water balance of soils. Relation between precipitation, evaporation and flow. *Ann. Agron.* **1954**, *5*, 491–569.
47. Jarsjö, J.; Shibuo, Y.; Destouni, G. Spatial distribution of unmonitored inland water discharges to the sea. *J. Hydrol.* **2008**, *348*, 59–72. [CrossRef]
48. SWECO International, Water Geosciences Consulting, Council for Geosciences and Water Resources Consultants. *SADC Hydrogeological Map and Atlas*; Water Division—SADC Infrastructure and Services Directorate: Gaborone, Botswana, 2010.
49. MacDonald, A.M.; Bonsor, H.C.; Dochartaigh, B.É.Ó.; Taylor, R.G. Quantitative maps of groundwater resources in Africa. *Environ. Res. Lett.* **2012**, *7*, 260–261. [CrossRef]
50. Weight, W.D.; Zaluski, M.; Sonderegger, J.L. *Manual of Applied Field Hydrogeology (Elektronisk Resurs)*; McGraw-Hill: New York, NY, USA, 2001.
51. Nicholson, S.; Yin, X. Rainfall conditions in equatorial East Africa during the nineteenth century as inferred from the record of Lake Victoria. *Clim. Chang.* **2001**, *48*, 387–398. [CrossRef]
52. Asokan, S.M.; Jarsjö, J.; Destouni, G. Vapor flux by evapotranspiration: Effects of changes in climate, land use, and water use. *J. Geophys. Res.* **2010**, *115*, 9–12. [CrossRef]
53. Törnqvist, R.; Jarsjö, J.; Pietroń, J.; Bring, A.; Rogberg, P.; Asokan, S.M.; Destouni, G. Evolution of the hydro-climate system in the Lake Baikal basin. *J. Hydrol.* **2014**, *519*, 1953–1962. [CrossRef]
54. Törnqvist, R.; Jarsjö, J. Water savings through improved irrigation techniques: Basin-scale quantification in semi-arid environments. *Water Resour. Manag.* **2012**, *26*, 949–962. [CrossRef]
55. Raes, D.; Mallants, D.; Song, Z. Rainbow—A software package for analysing hydrologic data. In *Hydraulic Engineering Software VI*; Blain, W.R., Ed.; Computational Mechanics Publications: Southampton, UK; Boston, MA, USA, 1996; pp. 525–534.
56. The Royal Netherlands Meteorological Institute (KNMI). Climate Explorer—Climate Change Atlas. De Bilt, The Netherlands. 2015. Available online: https://climexp.knmi.nl (accessed on 17 September 2015).
57. Intergovernmental Panel on Climate Change (IPCC). *Climate Change 2013: The Physical Science Basis. Contribution of Working Group I to the Fifth Assessment Report of the Intergovernmental Panel on Climate Change*; Cambridge University Press: Cambridge, UK; New York, NY, USA, 2013; p. 1535.
58. Dühnforth, M.; Bergner, A.N.; Trauth, M. Early holocene water budget of the Nakuru-Elmenteita basin, central Kenya Rift. *J. Paleolimnol.* **2006**, *36*, 281–294. [CrossRef]
59. Odada, E.; Olago, D.; Bugenyi, F.; Kulindwa, K.; Karimumuryango, J.; West, K.; Ntiba, M.; Wandiga, S.; Aloo-Obudho, P.; Achola, P. Environmental assessment of the East African Rift Valley Lakes. *Aquat. Sci.* **2003**, *65*, 254–271. [CrossRef]
60. Olaka, L.A.; Odada, E.O.; Trauth, M.H.; Olago, D.O. The sensitivity of East African Rift Lakes to climate fluctuations. *J. Paleolimnol.* **2010**, *44*, 629–644. [CrossRef]
61. Ayenew, T.; Becht, R. Comparative assessment of the water balance and hydrology of selected Ethiopian and Kenyan Rift Lakes. *Lakes Reserv. Res. Manag.* **2008**, *13*, 181–196. [CrossRef]
62. United Nations Environment Programme (UNEP). *World atlas of Desertification*; UNEP: London, UK, 1992.
63. Shanahan, T.M.; Overpeck, J.T.; Sharp, W.E.; Scholz, C.A.; Arko, J.A. Simulating the response of a closed-basin lake to recent climate changes in tropical West Africa (Lake Bosumtwi, Ghana). *Hydrol. Process.* **2007**, *21*, 1678–1691. [CrossRef]

64. Lyon, S.W.; Koutsouris, A.; Scheibler, F.; Jarsjö, J.; Mbanguka, R.; Tumbo, M.; Robert, K.K.; Sharma, A.N.; van der Velde, Y. Interpreting characteristic drainage timescale variability across Kilombero Valley, Tanzania. *Hydrol. Process.* **2015**, *29*, 1912–1924. [CrossRef]
65. Tessema, S.; Lyon, S.; Setegn, S.; Mörtberg, U. Effects of different retention parameter estimation methods on the prediction of surface runoff using the SCS curve number method. *Water Resour. Manag.* **2014**, *28*, 3241–3254. [CrossRef]